Topical Treatment for Cutaneous Leishmaniasis: Dermato-Pharmacokinetic Lead Optimization of Benzoxaboroles

Katrien Van Bocxlaer,[a] Eric Gaukel,[b] Deirdre Hauser,[b] Seong Hee Park,[b] Sara Schock,[b] Vanessa Yardley,[a] Ryan Randolph,[b] Jacob J. Plattner,[c] Tejal Merchant,[c] Simon L. Croft,[a] Robert T. Jacobs,[c] Stephen A. Wring[b]

[a]London School of Hygiene & Tropical Medicine, Faculty of Infections and Tropical Diseases, London, United Kingdom
[b]Scynexis Inc., Research Triangle Park, North Carolina, USA
[c]Anacor Pharmaceuticals, Inc., Palo Alto, California, USA

ABSTRACT Cutaneous leishmaniasis (CL) is caused by several species of the protozoan parasite *Leishmania*, affecting an estimated 10 million people worldwide. Previously reported strategies for the development of topical CL treatments have focused primarily on drug permeation and formulation optimization as the means to increase treatment efficacy. Our approach aims to identify compounds with antileishmanial activity and properties consistent with topical administration. Of the test compounds, five benzoxaboroles showed potent activity (50% effective concentration [EC_{50}] < 5 μM) against intracellular amastigotes of at least one *Leishmania* species and acceptable activity (20 μM < EC_{50} < 30 μM) against two more species. Benzoxaborole compounds were further prioritized on the basis of the *in vitro* evaluation of progression criteria related to skin permeation, such as the partition coefficient and solubility. An MDCKII-hMDR1 cell assay showed overall good permeability and no significant interaction with the P-glycoprotein transporter for all substrates except LSH002 and LSH031. The benzoxaboroles were degraded, to some extent, by skin enzymes but had stability superior to that of *para*-hydroxybenzoate compounds, which are known skin esterase substrates. Evaluation of permeation through reconstructed human epidermis showed LSH002 to be the most permeant, followed by LSH003 and LSH001. Skin disposition studies following finite drug formulation application to mouse skin demonstrated the highest permeation for LSH001, followed by LSH003 and LSH002, with a significantly larger amount of LSH001 than the other compounds being retained in skin. Finally, the efficacy of the leads (LSH001, LSH002, and LSH003) against *Leishmania major* was tested *in vivo*. LSH001 suppressed lesion growth upon topical application, and LSH003 reduced the lesion size following oral administration.

KEYWORDS *Leishmania*, benzoxaboroles, cutaneous leishmaniasis, pharmacokinetics, topical

The leishmaniases are a group of neglected tropical diseases that are caused by the obligate intracellular protozoan parasite *Leishmania* and that mainly occur in low- to middle-income countries. Leishmaniasis is endemic in 98 countries over five continents, placing 350 million people at risk of infection (1). Over 17 different *Leishmania* species can cause a variety of clinical symptoms that depend on both host- and parasite-related factors.

The most common form, cutaneous leishmaniasis (CL), is widely distributed, with 70 to 75% of the estimated cases occurring in Afghanistan, Algeria, Colombia, Brazil, Iran, Syria, Ethiopia, North Sudan, Costa Rica, and Peru (1), and continues to spread due to environmental changes, such as deforestation, travel, emigration, and agricultural practices (2–5). In its simplest form, CL presents as a single local skin lesion that tends

to heal spontaneously over a period of 3 to 18 months, leaving a scar (6). However, a range of clinical manifestations of variable severity is observed in patients that do not achieve spontaneous clearance of the parasite. These manifestations include nodules, ulcers, and plaques, depending upon the *Leishmania* species causing the infection and the status of the host's immune system (7). Immediate treatment is vital to expedite healing, reduce scar formation, prevent relapse, or prevent parasite dissemination.

Drugs commonly utilized to treat CL, such as pentavalent antimonials, miltefosine, amphotericin B, and paromomycin, are limited by parenteral drug administration, toxicity, variable efficacy, and cost. Over the past decade, despite efforts in screening and drug discovery to identify new chemical series for visceral leishmaniasis (8, 9), only a few novel chemical classes have been explored for CL. Instead, research mainly focused on repurposing existing drugs or novel formulation strategies. For example, amphotericin B, currently approved for parenteral delivery, has been evaluated for topical delivery in various formulations (10), including lipid nanocarriers (11, 12), nanoemulsions (13), or cyclodextrin complexes (14). Similarly, the antileishmanial drug paromomycin was formulated in conventional topical vehicles (15–18) and in novel delivery systems, including liposomes (19), in an attempt to increase skin permeation. However, the physicochemical properties of both drugs are unfavorable for skin permeation, and the reformulation strategies for these compounds have met with limited success.

To enable the further development of treatments for CL, we previously characterized how *Leishmania* infection impacts the permeability of the skin barrier and how this might influence topical drug delivery during the acute phase of the treatment (20). These studies have demonstrated that the skin barrier is compromised during the nodular stage of CL, suggesting a weaker barrier to dermal delivery.

Besides identifying disease-related changes to drug delivery, the identification of drug compounds that are active against a broad range of *Leishmania* parasites is also key (21). Benzoxaborole compounds, characterized by the boron atom incorporated in a ring system fused to an aromatic ring (Table 1), have previously been shown to have activity against bacteria, fungi, and protozoans, such as *Trypanosoma brucei* and *Plasmodium falciparum* (22–27). Phenotypic screenings of a library of benzoxaboroles identified the *in vitro* and *in vivo* activity of benzoxaborole 6-carboxamides against *T. brucei* and *T. cruzi*, the causative agents of human African trypanosomiasis (HAT) and Chagas disease (22, 28), respectively. Additionally, the activities of more than 2,000 compounds against *L. donovani* amastigotes were evaluated in THP-1 cells to identify drugs to treat visceral leishmaniasis and resulted in several hits with micromolar activity (DNDi-funded work, unpublished data).
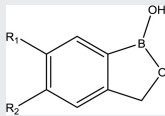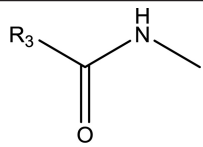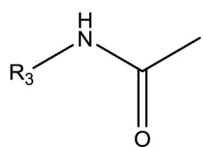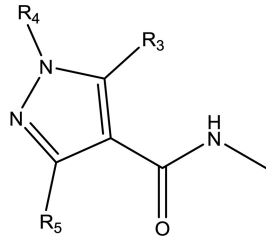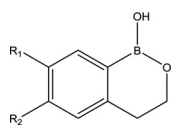
Here we describe an approach for the rational preclinical selection of candidate molecules for the treatment of CL (Fig. 1A), using a series of benzoxaboroles that (i) were found to demonstrate activity against a selection of *Leishmania* species, (ii) had the ability to permeate skin, and (iii) were appropriately distributed in various skin layers (Fig. 1B).

RESULTS

Structures of the compounds. Benzoxaborole compounds from four different chemical classes that had shown antiparasitic activity in the *P. falciparum*, *T. brucei*, *T. cruzi*, or *Leishmania donovani* screens were selected from the library for screening against CL-causing species. Some of the subclasses tested are shown in Table 1 and included benzoxaborole 6-carboxamides (subclass D), benzoxaborole 5-carboxamides (subclass B), pyrazole 6-carboxamides (subclass C), and benzoxaborininols (subclass E), in which the 5-ring structure containing the boron atom is replaced by a 6-ring structure.

***In vitro* antileishmanial activity.** Twenty-five compounds were screened against intracellular amastigotes. LSH001, LSH003, LSH023, LSH024, and LSH025 were the only five compounds that showed activity against at least one Old World species (*L. major*, *L. tropica*, and *L. aethiopica*) and one New World species (*L. mexicana* and *L. panamensis*)

TABLE 1 General structures of benzoxaboroles (subclass A) and subclasses benzoxaborole 6-carboxamides (subclass D), benzoxaborole 5-carboxamides (subclass B), pyrazole 6-carboxamides (subclass C), and benzoxaborininols (subclass E)

General benzoxaborole structure			
Chemical subclass	**Substituent**	**Modification**	**Compound identifiers**
Benzoxaborole 6-carboxamide	R1		LSH006, LSH009, LSH010, LSH011, LSH012, LSH015, LSH016, LSH019, LSH020, LSH021, LSH023, LSH024, LSH025
Benzoxaborole 5-carboxamide	R2		LSH002, LSH031
Pyrazole 6-carboxamides	R1		LSH022, LSH027, LSH028, LSH029
Benzoxaborininole			LSH001, LSH033
Other			LSH004, LSH005, LSH007, LSH013, LSH017, LSH018, LSH034

with 50% effective concentrations (EC$_{50}$s) below 30 μM (Table 2). These five test compounds were the most active against *L. tropica*, with an EC$_{50}$ below 5 μM, followed by *L. major*, with EC$_{50}$s in the same range. *L. mexicana* was the least susceptible species, with EC$_{50}$s for this species ranging from 9 to 22 μM. For most tested compounds, the EC$_{50}$ against *L. mexicana* was higher than 30 μM, the highest concentration tested, suggesting the low activity of the compound.

Amphotericin B, included as a positive control, had a high level of activity, with EC$_{50}$s ranging from 0.049 to 0.685 μM, indicating a 10-fold difference in sensitivity between *L. major*/*L. tropica* and *L. mexicana*. Miltefosine, the other control drug, was less active than amphotericin B, with the EC$_{50}$s ranging from 7 to 45 μM and 10 to 35 μM, respectively.

At this stage, it was decided to advance all compounds with potent activity (EC$_{50} <$ 5 μM) and/or moderate activity (5 μM $<$ EC$_{50} <$ 25 μM) against at least one Old World and one New World *Leishmania* species. Eight compounds (LSH026 to LSH034) with promising activity against other *Leishmania* species (DNDi, unpublished data) were also included in further assays.

Physicochemical properties. An initial computational screening of the test compounds was conducted to evaluate permeation-related physicochemical properties, i.e., the molecular mass, the presence of H-bond donors or acceptors, and the aqueous solubility. The partition coefficient was determined experimentally. It was found that
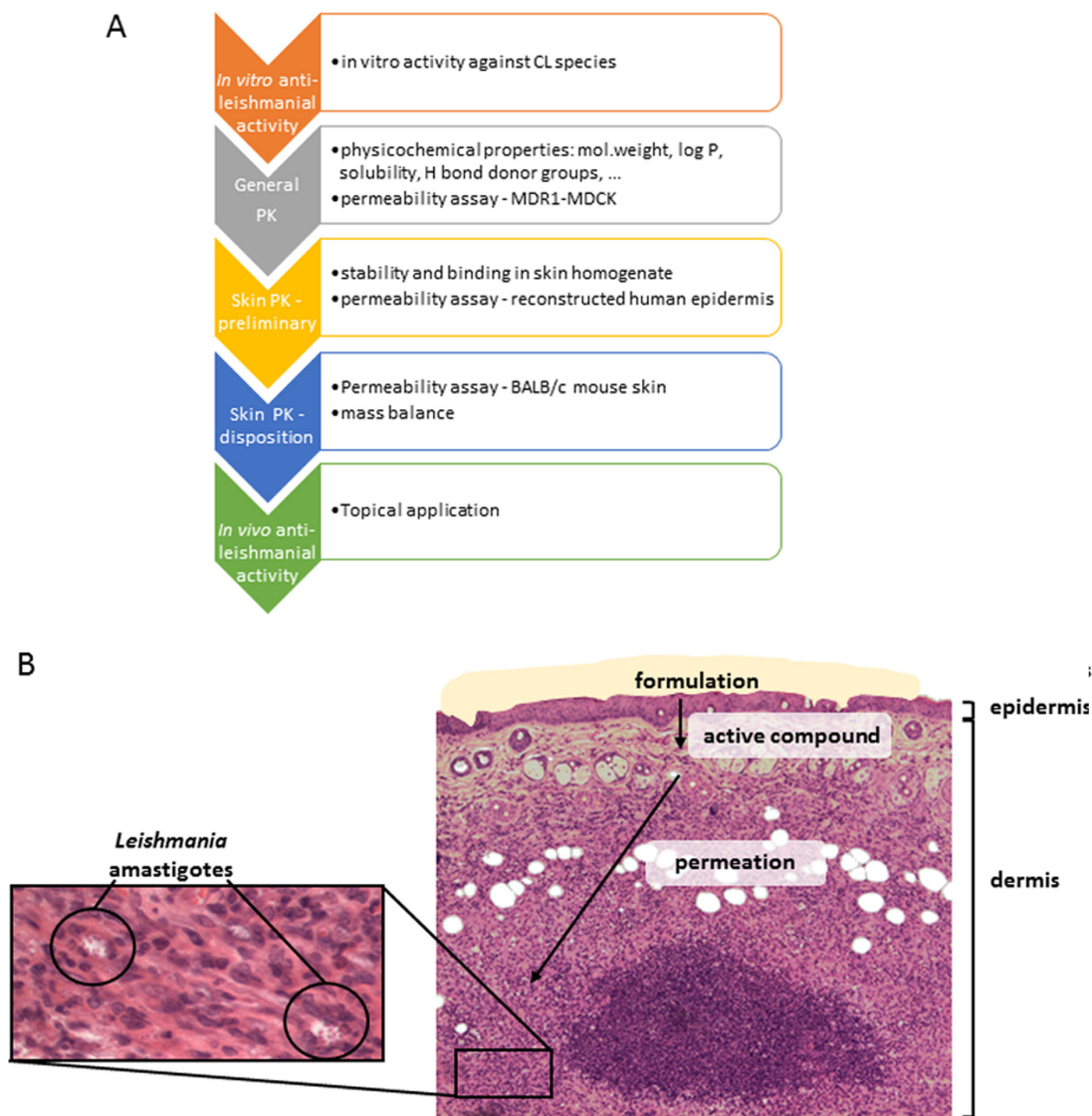
FIG 1 Drug delivery for CL. (A) Progression pathway during lead optimization of drugs as potential topical treatment for CL. (B) Histology of BALB/c mouse skin infected with *L. major*. The schematic (A) shows the route of the active drug through *Leishmania*-infected BALB/c mouse skin before reaching the *Leishmania* amastigotes situated in phagolysosome of dermal macrophages (B). PK, pharmacokinetics.

the benzoxaborole test compounds had appropriate physicochemical profiles for skin permeation (Table 3), i.e., a molecular mass below 500 g/mol, a log distribution coefficient (log *D*) value (at pH 7.4) of between 1 and 3 (except for LSH002 [log *D* = 0.44] and LSH032 [log *D* = 0.88]), and no more than 2 H-bond donor groups.

Intrinsic permeation. The MDCKII-hMDR1 cell assay was performed to identify the P-glycoprotein (Pgp) substrate and to evaluate the passive permeation of the test compounds across a simple epithelium, such as that of the intestine (29). The test compounds generally demonstrated high passive permeation (Table 4) in the assay, with values ranging from 247 to 688 nm/s (30) for all compounds except compound LSH002, which showed a low intrinsic permeation of 32.5 nm/s. Further, the absorptive quotient (AQ) value of only one compound (LSH002; AQ value, 0.492) exceeded the cutoff value (AQ, >0.3), indicating that it was a potential substrate for the efflux transporter Pgp. For comparison, amprenavir, the positive control included as a known Pgp substrate, afforded an AQ value of 0.846. Interestingly, the most active compounds during *in vitro* susceptibility studies all showed permeation values above 300 nm/s and were not Pgp substrates.

TABLE 2 Activity of benzoxaborole compounds against intracellular *Leishmania* amastigotes[a]

| Compound | n | EC$_{50}$ (95% CI) (μM) | | | | |
		L. tropica	*L. major*	*L. aethiopica*	*L. mexicana*	*L. panamensis*
Amphotericin B	1	0.066 (0.062–0.070)	0.043 (0.037–0.049)	0.115 (0.107–0.122)	0.430 (0.394–0.460)	0.143 (0.131–0.156)
	2	0.083 (0.078–0.089)	0.049 (0.043–0.056)	0.107 (0.096–0.119)	0.685 (0.553–0.692)	0.115 (0.093–0.142)
Miltefosine	1	19.99 (17.40–22.97)	44.85 (22.02–77.28)	7.79 (6.20–9.78)	31.04 (28.56–33.73)	19.98 (16.17–24.69)
	2	9.44 (7.78–11.45)	26.58 (21.30–33.15)	7.95 (7.26–8.69)	45.86 (36.61–57.45)	23.11 (20.41–26.18)
LSH001	1	2.01 (1.52–2.67)	4.26 (2.97–6.11)	22.10 (15.07–32.41)	23.04 (15.99–33.19)	18.82 (14.08–25.14)
	2	3.12 (2.38–4.09)	7.61 (5.48–10.57)	26.83 (19.40–37.11)	16.94 (9.62–29.83)	13.96 (10.06–19.44)
LSH002	1	14.96 (11.38–19.67)	16.52 (11.56–23.61)	>30	>30	>30
LSH003	1	2.46 (1.78–3.41)	3.93 (3.32–4.64)	11.12 (7.67–16.13)	18.94 (10.78–33.29)	8.09 (6.56–9.96)
	2	3.94 (2.96–5.25)	3.10 (2.25–4.26)	>30	>30	19.05 (15.03–24.16)
LSH004	1	16.08 (13.70–18.80)		29.97 (19.04–47.16)	>30	>30
LSH005	1	6.81 (5.84–7.94)		21.25 (13.18–34.26)	>30	>30
LSH006	1	>30		25.36 (15.88–40.50)	>30	>30
LSH007	1	5.71 (4.39–7.43)		27.18 (17.16–43.04)	>30	>30
LSH008	1	>30		>30	>30	>30
LSH009	1	3.08 (2.51–3.79)		17.66 (12.10–25.76)	>30	>30
LSH010	1	6.23 (5.49–7.06)	>30	11.71 (7.22–19.00)	>30	>30
LSH011	1	2.31 (1.73–3.08)	9.92 (8.49–11.59)	>30	>30	>30
LSH012	1	24.61 (14.31–42.30)	9.52 (6.80–13.32)	>30	>30	>30
LSH013	1	>30[b]	>30	>30	>30	>30
LSH014	1	5.91[b] (4.63–7.54)	4.15 (3.42–5.04)	>30	>30	29.59 (20.59–42.53)
LSH015	1	6.92 (4.95–9.66)	>30	>30	>30	>30
LSH016	1	5.40 (4.02–7.26)	>30	21.84 (14.60–32.66)	>30	>30
LSH017	1	>30	>30	>30	>30	>30
LSH018	1	>30	>30	>30	>30	>30
LSH019	1	21.01 (4.07–108.4)	>30	>30	>30	>30
LSH020	1	>30	>30	>30	>30	>30
LSH021	1	28.81 (17.03–48.74)	>30	>30	>30	>30
LSH022	1	>30	>30	>30	>30	>30
LSH023	1	1.19[b] (0.78–1.80)	1.57 (1.17–2.10)	23.05 (10.09–52.62)	6.31 (4.18–9.54)	2.98 (2.28–3.90)
LSH024	1	4.72[b] (3.31–6.74)	13.96 (11.52–16.91)	>30	>30	22.34 (17.66–28.25)
LSH025	1	2.21[b] (1.51–3.25)	5.93 (5.08–6.92)	>30	25.39 (15.81–40.78)	15.85 (12.85–19.56)

[a]n, number of experiment repeats; CI, confidence interval.
[b]*L. tropica* HTD4 instead of *L. tropica* AO21/p.

Previous research suggested an enhanced permeation of hydrophilic compounds in *Leishmania*-infected skin (20). Compounds LSH002 and LSH032 were therefore included in further assays, despite their less favorable physicochemical properties and/or intrinsic permeability.

Dermal stability, binding, and permeation. (i) Stability in skin supernatant. An initial rapid degradation of the test compounds was observed in skin supernatant

TABLE 3 Physicochemical properties of benzoxaborole compounds

Compound	Molecular mass[a] (g/mol)	H-bond donor groups/ H-bond acceptor groups[a]	Aqueous solubility[a] (μg/ml)	Log D (pH 7.4)[b]
Ideal skin permeant	<500	<3		1–3
LSH001	387	2/5	9	>2.63
LSH002	421	2/5	37	0.44 ± 0.06
LSH003	321	2/7	165	2.18 ± 0.08
LSH023	334	2/5	103	2.45 ± 0.04
LSH024	368	2/6	45	2.16 ± 0.07
LSH026	306	2/4	22	1.86 ± 0.07
LSH027	325	2/8	103	1.53[c]
LSH028	334	2/6	53	1.86 ± 0.02
LSH029	393	2/11	14	1.95 ± 0.10
LSH030	373	2/5	13	1.94 ± 0.06
LSH032	386	2/5	11	0.88 ± 0.15
LSH033	400	2/5	7	1.70 ± 0.15

[a]Data were obtained using ChemBioDraw Ultra (version 13.0) modeling software.
[b]Experimental data represent the mean ± SD (n = 3), unless indicated otherwise.
[c]Experimental data (n = 1).

TABLE 4 P_{app} values with and without GF918 and AQ for the MDCKII-hMDR1 cell assay

Compound	P_{app} (nm/s)		
	Without GF918	With GF918	AQ
Amprenavir	58.3	378	0.846
Propranolol	395	441	0.104
LSH001	583	599	0.027
LSH002	16.5	32.5	0.492
LSH003	626	635	0.014
LSH023	605	593	−0.020
LSH024	236	314	0.248
LSH025	322	349	0.077
LSH026	652	655	0.005
LSH027	209	247	0.154
LSH028	397	424	0.064
LSH029	229	268	0.146
LSH030	436	524	0.168
LSH032	232	327	0.291
LSH033	404	482	0.162
LSH034	543	538	−0.009

(Fig. 2) during the first 30 min, followed by slower drug metabolism. After 2 h, compound recovery was 25 to 60%, with LSH001, LSH002, LSH024, LSH025, LSH028, LSH031, LSH032, and LSH034 being moderately stable (amount remaining, 25 to 44%) and LSH003, LSH023, LSH026, LSH027, LSH029, LSH030, LSH033, and LSH034 being the most stable, with 45 to 75% of the test compound remaining. The two paraben compounds, ethyl paraben and propyl paraben, known substrates for skin esterases, were observed to break down very quickly in the presence of the skin supernatant. The recovery of these labile compounds was 10.9 and 0%, respectively, after 2 h of incubation.

(ii) Drug binding to skin components. A binding assay showed large variations in unbound fractions among the benzoxaboroles; unbound fractions ranging from 34% to 92% were observed (Table 5). Only 2 compounds, LSH001 and LSH026, had a high free fraction of 85% or more. The majority of the compounds had a free fraction of between
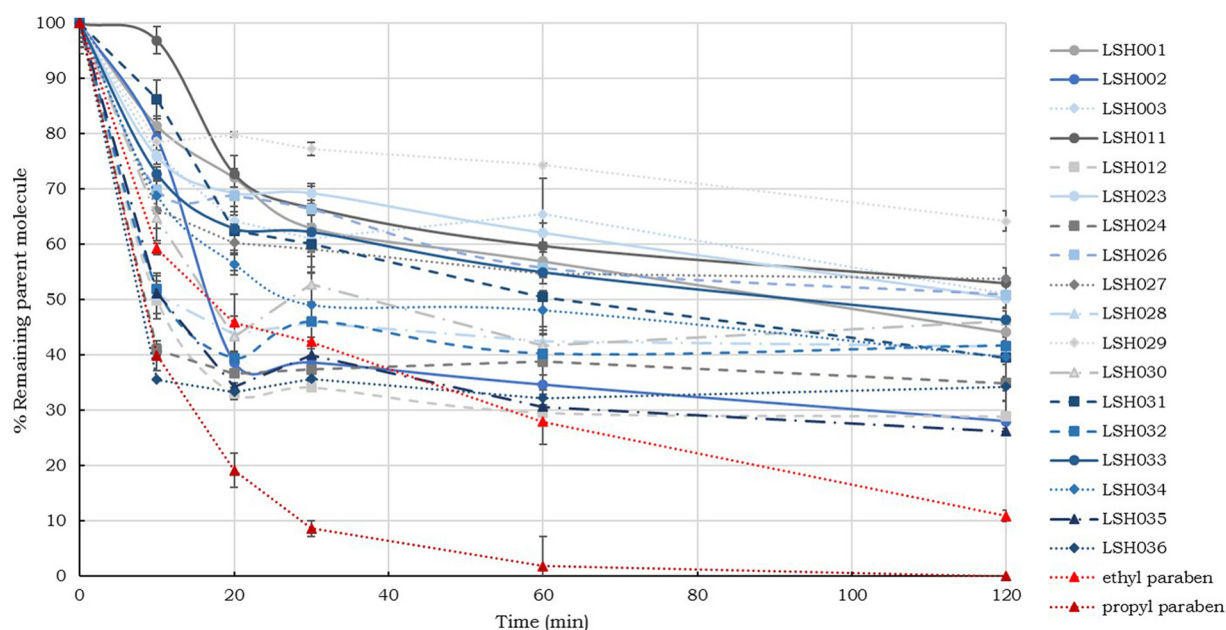

FIG 2 *In vitro* stability of the test compounds in skin homogenate. The fraction (in percent) of test compound remaining in the supernatant with a protein content of 2.5 mg/ml is shown as a function of time (mean ± SD, n = 3).

TABLE 5 Fractions of unbound compound and remaining compound after 2 h of incubation with mouse skin supernatant[a]

Compound	% unbound	% remaining test compound
Ethyl paraben		10.9
Propyl paraben		0.0
LSH001	87	44.1
LSH002	59	28.0
LSH003	44	51.0
LSH023	34	50.2
LSH024	50	35.0
LSH025	66	34.3
LSH026	92	50.8
LSH027	62	53.8
LSH028	60	41.5
LSH029	79	64.2
LSH030	67	46.2
LSH032	57	41.7
LSH033	65	46.3

[a]The stability of the compounds was measured at a protein concentration of 2.5 mg/ml.

50 and 85%, and finally, LSH003 and LSH023 had the lowest free fractions of 44 and 34%, respectively.

(iii) RHE permeation. Reconstructed human epidermis (RHE) was used to evaluate the passive permeation of the test compounds across multiple-layer membranes more representative of skin. The permeation of LSH002 was statistically significant higher than that of LSH001, LSH029, and LSH033 (one-way analysis of variance [ANOVA], $P <$ 0.05). As anticipated, the high-permeation hydrophilic control, caffeine, showed the highest permeation, which was significantly higher than that of all the test compounds and testosterone (lower-permeation, hydrophobic control) after 6 h (one-way ANOVA, $P < 0.05$). When ranking the cumulative amount that permeated over 6 h, the rank order from high to low was as follows: caffeine $>$ LSH002 $>$ LSH003 $>$ LSH023 $>$ testosterone $>$ LSH024 $>$ LSH033 $>$ LSH001 $>$ LSH029.

Both caffeine and LSH002 are more hydrophilic compounds, as indicated by their low log D values of -0.08 and 0.44, respectively. The vehicle in which all drugs were applied was ethanol-Miglyol 840 (1:9). Even though LSH002 was in solution, it might have been closer to saturation, exhibiting a higher thermodynamic activity than the other test compounds with a higher log D value. The higher permeation exhibited by LSH002 could also involve the higher affinity of this compound for RHE than for the lipophilic vehicle, thereby stimulating its preferential partitioning into the membrane.

On the basis of the overall data set collected, it was decided to select three compounds (LSH001, LSH002, and LSH003) for further study. LSH001 was included because it showed potent antileishmanial activity and was representative of a lipophilic compound, despite its lower permeation, which may prove helpful for formulation and skin disposition. LSH002 was included due to its higher solubility in water and, hence, its ability to be used as a control for disposition in the skin permeation assay, and LSH003 was selected because it was active against the five *Leishmania* species tested and it was ranked second with regard to flux in the permeation assay.

Dermal disposition. The objective of the first permeation study in mouse skin was to verify the rank order of the three selected compounds and compare that rank order with the results obtained from the previous permeation experiment where an RHE model was used (Table 6). Therefore, the experimental conditions and drug formulations were similar to those in the RHE experiment. The results are shown in Fig. 3 and indicate that the rank order LSH002 $>$ LSH003 $>$ LSH001 was maintained when using BALB/c mouse skin instead of the RHE membrane. Furthermore, the permeation of LSH002 through BALB/c mouse skin was significantly higher than that of LSH001, LSH003, and testosterone (one-way ANOVA, $P < 0.05$).

A second permeation study using BALB/c mouse skin aimed to assess the permeation and skin disposition of the compounds after application of a low volume of a 1%

TABLE 6 Permeation parameters: flux and lag time when using RHE and BALB/c mouse skin under the same conditions and BALB/c mouse skin when applying a low volume[a]

Strain	Testosterone		LSH001		LSH002		LSH003	
	Flux (ng/cm²/h)	Lag time (h)	Flux (ng/cm²/h)	Lag time (h)	Flux (ng/cm²/h)	Lag time (h)	Flux (ng/cm²/h)	Lag time (h)
RHE	28.0 ± 0.8	0.7 ± 0.1	21.8 ± 0.1	2.2 ± 0.1	143.9 ± 44.2	1.7 ± 0.8	45.1 ± 5.9	2.1 ± 0.1
BALB/c	2.2 ± 0.8	1.1 ± 0.6	6.6 ± 0.3[b]	2.4 ± 0.4	35.8 ± 0.9[b]	2.8 ± 0.3	8.0 ± 1.5[b]	2.5 ± 0.3
BALB/c Low vol			88.7 ± 8.8	2.7 ± 0.5*	13.5 ± 8.7[b]	2.7 ± 0.7	71.8 ± 18.0	2.7 ± 0.9

[a]Data represent the mean ± SD ($n = 3$), unless indicated otherwise.
[b]Data represent the mean ± SD ($n = 2$).

solution of test compound in ethanol-propylene glycol (E-PG) (1:1) solution (28 μl/cm²) comparable to that of the formulation intended for use in the murine CL model. Permeation (Table 5) was statistically significantly higher for LSH001 and LSH003 (one-way ANOVA, $P < 0.05$) than for LSH002. The rank order for flux was LSH001 > LSH003 > LSH002. Of note, in the E-PG formulation the more hydrophobic compounds (LSH001 and LSH003) achieved greater permeation than LSH002. No difference in the lag times of the different compounds was observed (ANOVA, $P > 0.05$).

A skin disposition study (Fig. 4) was conducted to compare the amount of test compound that either remained on the surface of the skin, was retained within the dermal layers, or had permeated through the skin. While there was no statistically significant difference between the amounts of compounds that had permeated over 24 h, the amount of LSH001 in the skin was significantly higher than that of LSH002 and LSH003 (one-way ANOVA, $P < 0.05$). The mass balance for total compound recovery was 84%, 87%, and 114% for LSH001, LSH002, and LSH003, respectively, indicating that an excellent mass balance was achieved for all compounds across the compartments.

***In vivo* antileishmanial activity.** After 10 days of topical application of the three selected compounds to the closed nodules, LSH001 halted the lesion size progression and the lesion sizes in this group were statistically significantly smaller than those in the vehicle control group (one-way ANOVA, $P < 0.05$), whereas no lesion size reduction was observed for LSH002 or LSH003 (Fig. 5A). The lesion sizes and parasite burden per lesion of the groups 3 days after the last drug administration are shown in Fig. 5B. The parasite load in the group receiving topical LSH001 was slightly lower than that in the other topically treated groups; however, there was no statistically significant difference (one-way ANOVA, $P > 0.05$).
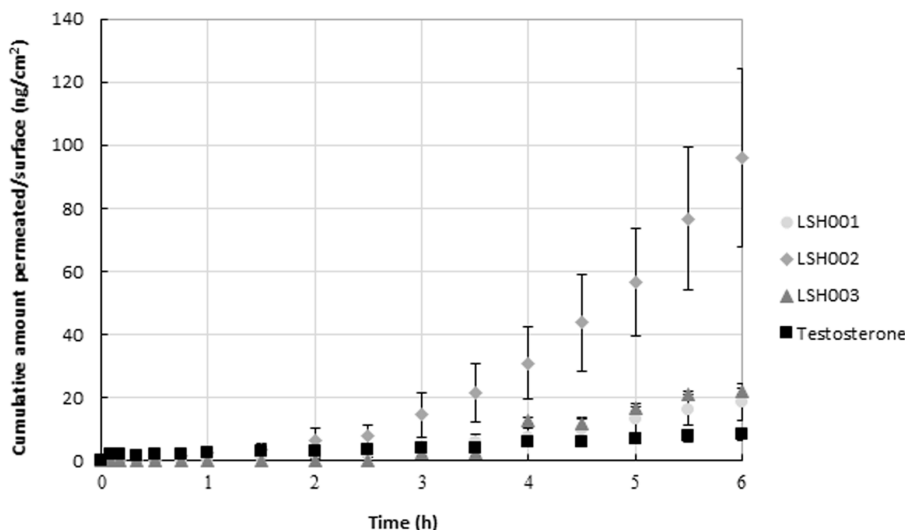

FIG 3 *In vitro* permeation through BALB/c mouse skin. The cumulative amount of LSH001, LSH002, and LSH003 that permeated over time was determined using Franz diffusion cells (mean ± SD, $n = 3$).
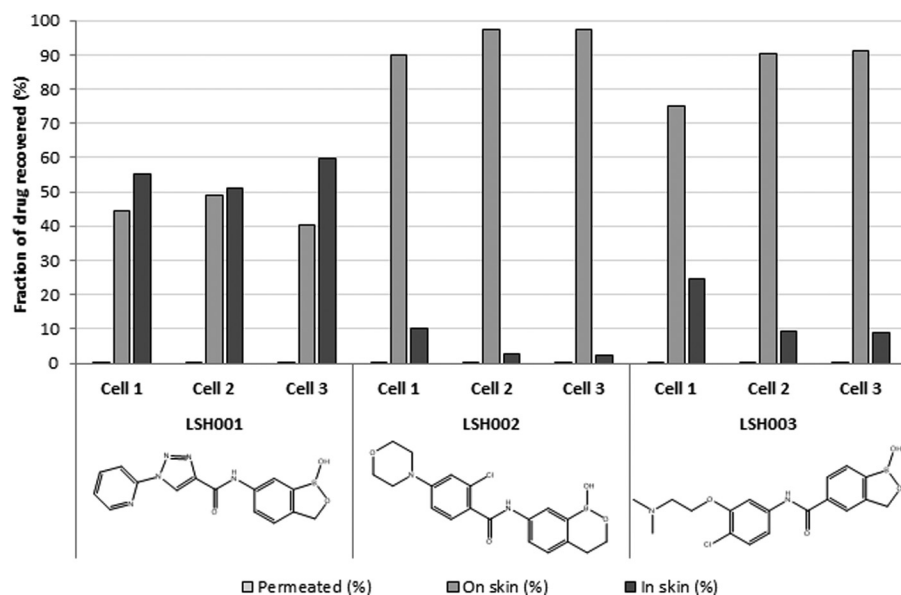
FIG 4 Skin disposition evaluation. The amounts of benzoxaboroles that permeated the skin or that were found in and on the skin are expressed as a percentage of the dosage retrieved.

While the primary aim of this work was to investigate the potential of benzoxaboroles for topical treatment for CL, the *in vitro* absorption, distribution, metabolism, and excretion (ADME) data suggest good overall permeability. Previous studies of the benzoxaboroles as orally active drugs for the treatment of HAT suggested good oral bioavailability for this class. Therefore, we administered the three test compounds LH001, LH002, and LH003 orally to mice with CL. A significant reduction of the lesion size was seen for the groups receiving LSH003 by the oral route compared to the lesion size for the relevant control group (one-way ANOVA, $P < 0.05$). This was also reflected in the parasite load, as the number of parasites per lesion was statistically significantly lower than that in the untreated control group (one-way ANOVA, $P < 0.05$).

For liposomal amphotericin B (AmBisome), the positive control, a statistically significant reduction in the lesion diameter and the parasite load compared to those in the control group was observed ($P < 0.05$), except for the groups receiving LSH001 topically and LSH003 orally ($P > 0.05$). This was expected, as previous reports described a reduction of both lesion size and parasite burden with amphotericin B (31).

DISCUSSION

Topical treatment for a dermatological infection limited to the more superficial layers of the skin offers an attractive alternative to the currently used routes of administration for CL treatment, as it (i) allows local drug targeting directly to the infection site, (ii) offers the potential to limit adverse effects, (iii) is not invasive, and (iv) is easy to apply by the patient. A systematic approach to the identification of potential lead compounds to progress to clinical trials is still lacking. The goal of this work was to explore a novel approach to identify promising compounds for the treatment of CL.

The benzoxaborole class of antiparasitics has demonstrated efficacy across multiple parasitic disease targets, including *Leishmania* spp. DNDI-6148 is at the preclinical stage of development for the treatment of visceral leishmaniasis (32), and oxaborole (SCYX-7158) is now in phase 2 clinical trials for the treatment of HAT (32). The goal of these programs was to identify orally active treatments for these systemic parasitic infections.

For successful therapeutic activity *in vivo* in CL, a drug requires both potent antileishmanial activity and an ability to permeate biological membranes in order to reach the *Leishmania* parasites in the dermal layer of the skin, a process that is impacted by both the physicochemical properties of the drug and the route of administration. Several criteria limit the delivery of drugs through the skin; drugs with a molecular
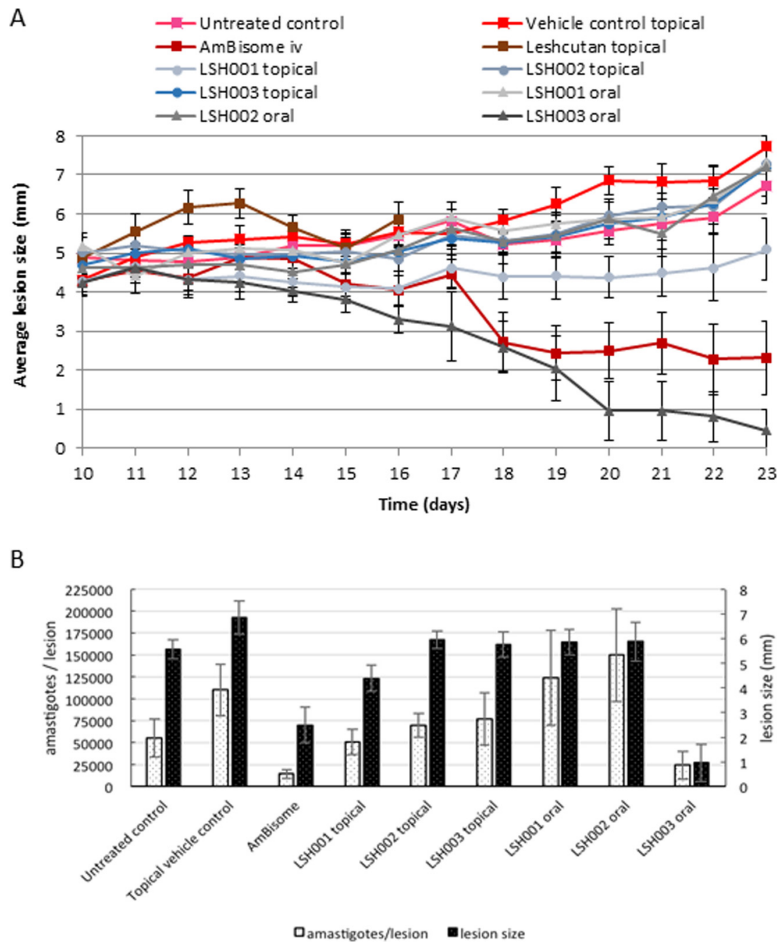
FIG 5 *In vivo* antileishmanial activity of benzoxaboroles upon oral and topical application. (A) Progression of the main lesion size (measured using digital calipers) per group as a function of time postinfection (mean ± SD, *n* = 6); (B) average number of amastigotes found per lesion, as analyzed by qPCR, and the average lesion size per group 3 days after the end of treatment (mean ± SD, *n* = 5). iv, intravenous.

mass of <500 g/mol (33), a partition coefficient of between 1 and 3 (34, 35), a low melting point (<200°C) (36), an aqueous solubility of >1 mg/ml (37), and less than 2 H-bond donor groups (38) are more likely to permeate the skin. Topically applied drugs also undergo relatively little enzymatic degradation compared to orally administered drugs, which need to pass a monolayer of intestinal epithelium and have low hepatic first-pass metabolism before they reach the blood circulation to allow distribution to the skin (35).

While each layer of the skin is a potential hurdle to drug permeation, it is the outer layer of the skin, the stratum corneum, that is a highly restrictive permeability barrier, formed of 10 to 15 layers of dead keratinized cells imbedded in an intercellular lipid mixture organized in bilayers (39, 40). This inherent difference between biomembranes governs the preferential permeation of certain drugs (35).

Previously reported strategies for developing topical treatments for CL have focused solely on formulation optimization as a means to increase treatment efficacy, whereas we wish to identify compounds with intrinsic properties consistent with topical administration. To achieve this objective, we systematically evaluated physiologically based pharmacokinetic parameters and aimed to correlate these to the physicochemical properties of the compounds. A diverse set of benzoxoboroles associated with good drug-like properties in previous antiparasitic programs was selected. The compounds were assessed for their likely intrinsic activity against Old and New World species

causing CL by measuring the *in vitro* activity against the intracellular amastigote form using a previously reported assay (41).

Dermal drug-like properties were characterized by comparing physicochemical properties, *in vitro* permeation through MDCKII-hMDR1 cells and RHE models, and stability in skin homogenate. Subsequently promising compounds were advanced to a whole-skin permeability, binding, and disposition evaluation. This strategy of selection was employed to advance the most promising compounds to the more complex assays. Ultimately, this strategy identified three compounds, each of which had unique features, for evaluation in a murine model of CL.

Initially, five benzoxaborole 6-carboxamides showed broad-range activity against CL-causing species. To complement this intrinsic activity, *in vitro* membrane permeation assays were employed to assess each compound's ability to cross a cellular barrier. Previously, the MDCKII-hMDR1 cell transwell assay was successfully utilized to classify compounds with a potential high level of permeation across the gut when the apparent permeation (P_{app}) in the presence of GF918 ($P_{app\ +\ GF918}$) value from the apical to the basolateral side was >50 nm/s (42) or the blood-brain barrier when the $P_{app\ +\ GF918}$ value from the apical to the basolateral side was >150 nm/s and the compound was a non-PgP substrate (43). While for dermal permeation no clear selection criteria were found in the literature, our test compounds generally exhibited high permeation, with a $P_{app\ +\ GF918}$ value from the apical to the basolateral side of >200 nm/s, except for LSH002 ($P_{app\ +\ GF918}$ value from the apical to the basolateral side = 32.5 nm/s). Furthermore, the MDCKII-hMDR1 cell assay allowed us to identify potential substrates of the P-glycoprotein (Pgp) efflux transporter (44–46) which is helpful, considering that these compounds may suffer from a reduced fraction absorbed following oral delivery (47, 48) but may also demonstrate a reduced ability to penetrate macrophages. This is important because *Leishmania* parasites survive and divide inside macrophages, meaning that drugs that are Pgp substrates might potentially be less active than drugs that are not Pgp substrates, as efflux would attenuate entry into macrophages (49, 50). In fact, reports of the inactivity of antimonial drugs against *L. donovani* in patients were linked to the upregulation of Pgp transporters in the host cells, leading to low concentrations of drug in the macrophages and, thus, disease progression (51). In our set of test compounds, only LSH002 showed an absorption quotient higher than 0.3, indicating that it potentially is a Pgp subtrate (42).

Moving on from the cellular models of permeation, the permeation of the test compounds was further evaluated in the complex RHE, which has shown the ability to predict dermal permeation (52), allowing us to further rank order our test compounds. The hydrophilic compounds caffeine and LSH002 showed the highest permeation in this model. Caffeine and LSH002 were the most hydrophilic compounds among the test compounds, as was indicated by their log *D* values of −0.08 and 0.44, respectively. Hence, even though LSH002 was in solution, it might have been closer to saturation in the ethanol-Miglyol 840 (1:9) vehicle, exhibiting a higher thermodynamic activity than the test compounds with higher log *D* values. The second highest permeation was observed for LSH003, the test compound that also showed good *in vitro* antileishmanial activity against all five *Leishmania* species. LSH001, also active *in vitro* against all *Leishmania* spp., showed a slightly lower permeation than testosterone, the lipophilic control drug.

When evaluating the permeation of these three compounds in BALB/c mouse skin using the same experimental design, the overall permeation and, thus, flux of the test compounds and testosterone were lower than the permeation through RHE (one-way ANOVA, $P < 0.05$) (Table 3). Several studies have indicated that RHE is more permeable than animal and human skin (53–55). The rank order of the test compounds' permeation through mouse skin was the same as that for permeation through RHE (LSH002 > LSH003 > LSH001), and more importantly, the permeation of all test compounds was higher than that of testosterone.

We next explored the metabolic stability of the benzoxaboroles in both liver-based and skin-based assays. Degradation of drugs in the skin has been reported (56–58), with

the main site of activity being situated in the epidermis (59). We used the supernatant of skin homogenate to determine the drug stability and observed that all benzoxaborole test compounds showed a higher stability than the paraben compounds, which are known substrates for skin esterases and are therefore expected to break down (60). The fraction of parent compound remaining after 2 h of incubation was relatively similar for all compounds and ranged from approximately 30 to 60%. The skin homogenate was prepared using full-thickness BALB/c mouse skin as opposed to epidermal membranes alone. Epidermal membranes exhibited reduced enzymatic activity compared to full-thickness skin (61), possibly due to the exposure to heat required to separate the epidermal and dermal membranes. Furthermore, the *in vivo* efficacy study will be conducted in female BALB/c mice, and thus, full-thickness mouse skin was used to ensure consistency between the *in vitro-in vivo* data set. During the preparation of our homogenate, intracellular enzymes contributing to the breakdown of drugs might have been released, in which case these results represent an overestimation of drug metabolism (58). How these results compare to those with human skin is unclear, but a study comparing paraben breakdown in rat and human skin observed a higher metabolism, on the order of magnitudes, for rat skin, indicating that the level of breakdown in human skin is expected to be lower than the results obtained here (62).

Drug binding to skin proteins can also result in the inability of the drug to reach or distribute to its target; it is the unbound (free) fraction of the drug in the dermis that is pharmacologically active, as it can passively permeate into the macrophage and from there into the parasite (63). After incubation in skin homogenate, our test compounds exhibited a range of unbound fractions. A certain level of drug-skin binding is desirable to establish a depot effect, leading to the slow release of the drug from the skin into the macrophage and *Leishmania* parasite. As the unbound fractions across a membrane are in equilibrium, drug being taken up by the macrophage will cause drug bound to skin components to be released and become available for uptake into the macrophage. Moreover, the skin binding could prevent systemic exposure and, therefore, preliminary drug metabolism and excretion.

Prior to *in vivo* evaluation, the skin disposition of the compounds was evaluated using BALB/c mouse skin under real-life conditions, e.g., a limited volume of a 1% (wt/vol) test compound formulation. This showed a lower permeation for LSH002 than for LSH001 and LSH003, in contrast to the higher permeation shown for LSH002 in RHE. This is likely due to the change in vehicle and, thus, saturation therein. LSH001 and LSH003 were applied as suspensions with a maximal thermodynamic activity, while LSH002 was applied as a solution at about 80% saturation and, thus, a suboptimal thermodynamic driving force. Also due to its hydrophilic nature, LSH002 is likely to have a higher affinity for the E-PG vehicle than for the skin, causing the drug to remain in the vehicle on the skin surface. In addition, our mass balance data showed a significantly lower drug fraction in the skin for both LSH002 and LSH003 than for LSH001 (one-way ANOVA, $P < 0.05$). For LSH001, about half of the applied drugs permeated into the skin. LSH001 has a high log D, which is expected to facilitate partitioning and diffusion into the stratum corneum. A high log D, however, is unfavorable for permeation into the dermis.

When evaluating the activity of these test compounds *in vivo*, LSH001 applied topically was able to halt the lesion growth, which suggests that the drug was able to permeate through the stratum corneum and reach the parasites situated in the lower epidermis and dermis. LSH003 administered orally significantly reduced the lesion size and parasite burden compared to the lesion size and parasite burden reductions achieved with LSH001 and LSH002 administered orally. This nonhealing BALB/c mouse model is a rigorous test for drugs because (i) upon infection with *Leishmania* parasites, the mice develop fulminating infections with ulcers that quickly progress to death if left untreated (64) and (ii) the drugs were applied only after establishment of the lesions. For this model, lesion size reduction or suppression of lesion growth is regarded as a promising result (64).

The determination of efficacy of the topical formulations can be difficult to gauge,

as the mice are able to remove the formulation by licking the site. For LSH001, there was no change in lesion progression when the compound was administered orally. This suggests that the drug that permeated the skin exerts the suppression of nodule growth observed upon topical application of the same agent. This correlates with the data obtained from the *in vitro* permeation experiment using BALB/c mouse skin. Not only did LSH001 show a higher permeation than LSH002 and LSH003, but also the mass balance study showed a statistically higher concentration of LSH001 than the two other test compounds in the skin. Of the three compounds tested *in vivo*, LSH001 also exhibited the highest unbound fraction. It could be hypothesized that even for topical compounds it is beneficial to have a high unbound fraction in order to exert antileishmanial activity, as opposed to binding to skin.

LSH001 suppressed nodule growth when applied topically, whereas oral administration with the same agent did not affect lesion size. The opposite results were found for LSH003, whereby oral administration reduced the lesion size but topical administration had no effect. Since LSH001 and LSH003 exhibited the same *in vitro* activity against *L. major*, it is thus suggested that the difference in efficacy upon oral administration is due to pharmacokinetic variations between LSH001 and LSH003.

Conclusions. Previously, the process of development of drugs for the treatment of CL mainly focused on drug activity testing and formulation optimization. Current *in vitro* models to test antileishmanial activity rely on two-dimensional culture systems that demonstrate activity against the intracellular parasite but whose results correlate poorly with the results obtained in animal models (65). This disconnect is likely caused by the oversimplification of the *in vitro* model, which is unable to account for the pharmacokinetic drug barriers that occur *in vivo*.

We have shown that a more complete evaluation of a drug candidate is established by incorporating physiologically based pharmacokinetic assays in our drug discovery, leading to an improved selection of lead candidates, which is essential to improve the likelihood of success of clinical candidates (66, 67).

Furthermore, this stepwise approach allows evaluation of the test compounds at each stage and enables input from medicinal chemistry to alter the core molecule to optimize the physicochemical properties to increase the distribution and specificity of the drug in the skin at an early stage of development.

MATERIALS AND METHODS

Materials. The compounds were synthesized by Anacor Pharmaceuticals, Inc., and Scynexis Inc. (Research Triangle Park, NC) and were of >95% purity, as determined by high-performance liquid chromatography (HPLC), liquid chromatography (LC)-mass spectrometry (MS), and ^{1}H nuclear magnetic resonance analyses. Stock solutions (1 mM) were prepared in dimethyl sulfoxide (DMSO) for use in the *in vitro* experiments. HPLC-grade solvents were purchased from Fisher Scientific (Pittsburgh, PA). Formic acid (≥98% purity; Fluka), caffeine, testosterone, 1-octanol, and high-grade vacuum silicone grease (Dow Corning) were acquired from Sigma-Aldrich (St. Louis, MO). Ammonium formate (99% purity; Alpha Aesar) was purchased from VWR International, LLC (West Chester, PA). Miglyol 840 (propylene glycol dicaprylate/dicaprate) was obtained from Sasol Germany GmbH (Witten, Germany). Phosphate-buffered saline (PBS), as well as Dulbecco's modification of Eagle's medium with GlutaMAX, trypsin-EDTA, and fetal bovine serum, was supplied by Gibco (Invitrogen Corporation, Carlsbad, CA). Penicillin-streptomycin solution, Hanks' balanced salt solution, and HEPES buffer were obtained from Sigma-Aldrich.

Mice. Female BALB/c mice (6 to 8 weeks old) were purchased from Charles River (Margate, UK) and housed in a controlled environment of 55% relative humidity and 26°C. Tap water and a standard laboratory diet were provided *ad libitum*. All *in vivo* experiments were carried out under license (PPL 70/8207) at the London School of Hygiene & Tropical Medicine (LSHTM) after discussion with the veterinarian and clearance through the LSHTM Animal Welfare and Ethical Review Board and according to UK Home Office regulations.

Parasite and cell maintenance. *L. major* (MHOM/SA/85/JISH118), *L. panamensis* (MHOM/PA/67/BOYNTON), *L. aethiopica* (MHOM/ET/84/KH), *L. mexicana* (MNYC/BZ/62/M379), and *L. tropica* (MHOM/IR/2013/HTD4 and AO21/p) were routinely passaged through BALB/c mice, and low-passage-number number promastigotes (typically, below passage number 3) were used for the assays. All promastigotes, except for *L. panamensis* and *L. aethiopica* promastigotes, were maintained in Schneider's insect medium (Sigma-Aldrich, UK) supplemented with 10% heat-inactivated fetal calf serum (HiFCS; Harlan, UK) at 26°C. M199 medium supplemented with 10% HiFCS was used for the latter two strains.

MDCKII-human MDR1 cells (Netherlands Cancer Institute, Amsterdam, Netherlands) were maintained in Dulbecco's modified Eagle's medium (DMEM), and KB cells were maintained in RPMI 1640 medium

supplemented with L-glutamine and 10% HiFCS. Both human-derived cell lines were left in an incubator at 37°C in 5% CO_2 and passaged to new medium once a week (1/10 ratio).

***In vitro* antileishmanial activity.** Mouse peritoneal macrophages (PEMs) were isolated from CD-1 mice (Charles River, Margate, UK) by abdominal lavage with RPMI 1640 medium containing 1% penicillin and streptomycin. The collected cells were washed, resuspended, and seeded in a 16-well Lab-Tek slide in RPMI 1640 medium supplemented with 10% HiFCS at a density of 4×10^4 per well. After 24 h of incubation at 37°C in a 5% CO_2–95% air mixture, the adhered PEMs were infected with stationary-phase promastigotes at a ratio of 3 (for *L. tropica* and *L. major*) or 5 (for *L. mexicana*, *L. aethiopica*, and *L. panamensis*) promastigotes to 1 macrophage and maintained at 34°C in a 5% CO_2–95% air mixture. These inoculum ratios were chosen to achieve at least 75% infection of untreated control macrophages after 72 h of incubation.

After 24 h, the cultures were washed to remove extracellular promastigotes, and one slide was fixed with methanol and stained with Giemsa to determine the initial level of infection. If a sufficient level of infection was obtained, experimental drug solutions over a range of concentrations of 30, 10, 3, and 1 μM were added in quadruplicate at each concentration. Amphotericin B (Fungizone) and miltefosine were included as control drugs. After 72 h of incubation, all slides were methanol fixed and Giemsa stained.

The percent inhibition was determined by counting the infected macrophages in drug-treated cultures under a microscope (magnification, ×400), and the count was compared to that in the untreated cultures. The Hill coefficient and EC_{50} and EC_{90} values were calculated by nonlinear sigmoidal curve fitting (variable slope) using Prism software (GraphPad, Surrey, UK).

***In vitro* ADME studies: general pharmacokinetic predictions.** Descriptors of the test compounds consisting of molecular mass, aqueous solubility, and the number of H-bond donors and acceptors present were calculated using ChemBioDraw Ultra software (version 13.0; PerkinElmer, Waltham, MA).

Distribution coefficient. The 1-octanol phase was left to saturate with PBS (pH 7.4) on a shaking plate at 32°C for 48 h. The test compounds were then dissolved in the 1-octanol at a concentration of 1 μg/ml and left to equilibrate with an equal volume of PBS on a shaking plate at 32°C for 48 h. The 1-μg/ml concentration was selected such that the amount of the candidate drug in each phase did not exceed 10% of the solubility limit of that compound. Aliquots of each phase were taken and diluted in the mobile phase followed by LC-tandem MS (MS/MS) analysis. Each experiment was conducted in triplicate. The log distribution coefficient (log D) was calculated as shown in equation 1:

$$\log D\,(\text{pH 7.4}) = \log\left[\frac{[\text{solute}]_{\text{oct}}}{[\text{solute}]_{\text{pbs}}^{\text{ion}} + [\text{solute}]_{\text{pbs}}^{\text{neutral}}}\right] \tag{1}$$

where $[\text{solute}]_{\text{oct}}$ is the 1-octanol solute concentration, $[\text{solute}]_{\text{pbs}}^{\text{ion}}$ is the concentration of solute in its ionized form in PBS, and $[\text{solute}]_{\text{pbs}}^{\text{neutral}}$ is the concentration of solute in its un-ionized form in PBS.

***In vitro* prediction of permeation and Pgp-mediated efflux transport.** MDCKII-hMDR1 cells were seeded in the apical chamber of a 12-well Transwell plate (Corning Inc., Lowell, MA) at a density of 6.6×10^6 cells/well, and 1.5 ml of medium was applied in the basolateral chamber. After 24 h, nonadhered cells were washed away and new medium was applied to both chambers. The cells were incubated for an additional 48 h at 37°C to form confluent monolayers.

Prior to the addition of the test compounds, the cell culture medium was removed and replaced with transport medium consisting of Hanks' balanced salt solution with 24 mM glucose and 24 mM HEPES buffer. The integrity of the monolayers was ensured by measuring the transepithelial resistance (TEER) for each insert (TEER > 160 Ω cm²). Assays were performed in triplicate by adding 3 μM drug solutions (1 mM DMSO stock solutions diluted in transport medium) in the absence or presence of 2 μM GF918 (a potent Pgp inhibitor [68]) in the transport buffer of the apical chamber. The comparator controls propranolol and amprenavir for transcellular transport and Pgp efflux, respectively, were included in each assay. The Transwell plates were incubated on a shaking plate (160 rpm) at 37°C in 5% CO_2 for 1 h. After incubation, aliquots from both chambers were removed for analysis by LC-MS/MS.

Values for mass balance, apparent permeation (P_{app}) from the apical to the basolateral side (equation 2), the apparent permeation value from the apical to the basolateral side in the presence of GF918 ($P_{\text{app + GF918}}$), and the absorption quotient (AQ) (equation 3) were calculated for each compound (30, 42, 69). Test compounds with an AQ of ≤0.3 were considered non-Pgp substrates, while compounds with an AQ of >0.3 were considered Pgp substrates (30, 42). The acceptance criterion for mass balance was 70 to 120%.

$$P_{\text{app}} = \frac{dQ/dt}{C_o \times A} \tag{2}$$

$$AQ = \frac{P_{\text{app + GF918}} - P_{\text{app}}}{P_{\text{app + GF918}}} \tag{3}$$

where AQ is absorption quotient, t is time, C_0 is the initial concentration, and A is area.

Analysis of test compounds in biological samples. (i) Skin tissue homogenization. For the preparation of the skin homogenates, 20 ml of ice-cold Dulbecco's modified PBS (pH 7.4) was added to fine pieces of approximately 2 g of shaved dorsal full-thickness BALB/c mouse skin (Bioreclamation LLC, Westbury, NY). The tissue suspension was homogenized using an Omni probe homogenizer (Kennesaw, GA) and centrifuged for 10 min at 800 × *g* to sediment cellular residue. The protein content of the supernatant was determined using a Pierce bicinchoninic acid protein assay kit (Pierce, Rockford, IL) and adjusted to 2.5 mg/ml. The supernatant was stored at approximately −80°C until use.

(ii) LC-MS/MS. Sample analysis was performed by liquid chromatography-tandem mass spectrometry (LC-MS/MS). The instrumentation consisted of a CTC Pal autosampler (Leap Technologies, Carrboro,

TABLE 7 Summary of experimental conditions for different permeation experiments

Permeation expt	Compounds	Donor vehicle	Concn (μg/ml)	Vol/skin surface area (μl/cm²)
RHE 1	LSH001, LSH003, LSH011, LSH012, LSH023, LSH024, LSH029, LSH034, caffeine, testosterone	Ethanol-Miglyol 840 (1:9), except for caffeine	100	300
FDC 1	Mix 1 (LSH001, LSH002), mix 2 (LSH003, LSH034)	Ethanol-Miglyol 840 (1:9)	100	300
FDC 2	LSH001, LSH002, LSH003	Ethanol-PG (1:1)	10,000[a]	28.4

[a]One percent (wt/vol).

NC), two Agilent 1100 series pumps (Agilent Technologies Inc., Santa Clara, CA), a CH-30 column heater (Eppendorf, Hauppauge, NY), and an API 3000 triple-quadrupole mass spectrometer (Applied Biosystems, Foster City, CA) equipped with a turbo-ion electrospray interface for detection. Chromatography was performed on a Luna C_{18} reversed-phase column (50 by 2 mm; particle size, 3 μm) from Phenomenex (Torrance, CA) protected by a matched-phase guard column. The mass spectrometer and peripheral devices were controlled using Analyst software (version 1.4.2; Applied Biosystems, Foster City, CA). The mobile phase used to elute the compounds consisted of 5 mM ammonium formate and 0.1% (vol/vol) formic acid in water (mobile phase A) and 5 mM ammonium formate and 0.1% (vol/vol) formic acid in methanol mobile phase (B). The samples were introduced onto the column using 90% mobile phase A at a flow rate of 600 μl/min, followed by a step gradient to 90% mobile phase B between 0.5 and 1 min. For analytical chromatography, a linear gradient of 10% mobile phase A was maintained for 2 min, after which the mobile phase was switched back to 90% mobile phase A. This mobile phase composition was maintained until the end of the run (3.5 min). Test compounds eluted between 2 and 3 min.

***In vitro* stability and disposition in skin homogenates. (i) Stability in skin homogenates.** The stability of the compounds was measured at a protein concentration of 2.5 mg/ml. Each compound (10 μM) was incubated in mouse skin homogenate on a shaking plate at 32°C. An aliquot of the incubation mixture was collected at 0, 10, 20, and 30 min, 1 h, and 2 h and quenched with 4 volumes of ice-cold methanol containing 0.1% formic acid. Samples were centrifuged at 3,000 $\times$ *g* for 10 min at 15°C, and the obtained supernatant was analyzed for the test compound by LC-MS/MS. Ethyl paraben and propyl paraben, ester compounds known to undergo degradation due to enzymatic hydrolysis to yield hydroxybenzoic acid, were included as positive controls.

(ii) Skin tissue binding. Rapid equilibrium dialysis (RED) devices (Pierce, Rockford, IL) in plate format were used to determine drug binding to the skin homogenate supernatant. A day prior to the experiment, the Teflon plate was washed with 30% ethanol and rinsed twice with deionized water before it was left it to dry. On the day of the experiment, skin supernatant was thawed and the test compound was added to a final concentration of 10 μM. Samples of fortified skin tissue homogenate (300 μl) were added to the sample chambers of the RED devices, and PBS (500 μl; Pierce, Rockford, IL) was added to each buffer chamber. Plates were incubated on a shaking plate at 32°C for 2 h. Aliquots of both phases were collected and treated with 4 volumes of ice-cold methanol with 0.1% formic acid to precipitate the proteins. Treated sample aliquots were centrifuged at 3,000 $\times$ *g* and 15°C for 10 min. The resulting supernatants were assayed for the parent drug concentration by LC-MS/MS.

(iii) *In vitro* prediction of skin permeability. EpiDerm skin model EPI-606-X was obtained from MatTek Corporation (Ashland, MA, USA). The EPI-606-X model is characterized by an enhanced barrier function and was specifically designed to conduct permeability assays. Upon receipt, the skin tissue (lot 17860) was stored overnight at 2 to 8°C. On the day of the experiment, the skin inserts were transferred to a 6-well plate containing 2 ml of Dulbecco's modified PBS and left to acclimatize on a heated shaking plate. The temperature was set at 36.6°C, which corresponded to a skin temperature of 32°C.

Due to low water solubility, the test compounds were prepared in an ethanol-Miglyol 840 (1:9) vehicle, a solution that has been used for permeation studies with poorly soluble drugs (70). After 1 h, 1.14 ml of a 100-μg/ml donor solution was applied on the model skin using a positive-displacement pipette. The plates were left to incubate with gentle shaking at 95 rpm. Caffeine (log D = −0.08) and testosterone (log D = 3.32) were included as control comparator compounds in each assay run. Each control was evaluated at the same concentration as the test compounds. Testosterone, representing a hydrophobic control, was formulated in the ethanol-Myglyol 840 vehicle, and caffeine, representing a hydrophilic control, was prepared in Dulbecco's modified PBS. Aliquots were removed from the receiver fluid of each chamber and replaced with fresh PBS at regular time points over the course of 6 h of incubation. The samples were assayed for test compound by LC-MS/MS. The permeation of each compound was evaluated in triplicate. Statistical analyses were performed using SPSS software (version 19.0).

Skin disposition. (i) *In vitro* permeation prediction using full-thickness BALB/c mouse skin. *In vitro* permeation studies were conducted in a semiautomated system comprising 6 water-jacketed, static, vertical-type Franz diffusion cells (FDC) from Logan instruments Ltd. (Somerset, NJ). The permeation studies had two objectives (Table 7). The first objective was to compare the permeation of the test compounds through BALB/c mouse skin to the permeation determined by means of the RHE assay. Therefore, the experimental conditions were held to be consistent with those employed for the RHE assay. The second objective was to compare the permeation of the test compounds using the formu-

TABLE 8 Summary of the different *in vivo* experimental groups with their treatment regimens[a]

Group	Formulation	Active compound	Vehicle	Administration route	Treatment regimen
1	Untreated control	None	None	None	None
2	AmBisome	Amphotericin B	Dextrose (5%)	Intravenous	25 mg/kg of body wt b.i.d., 5 doses
3	Leshcutan	Paromomycin sulfate (15%)	Methylbenzethonium chloride (12%) in petrolatum	Topical	0.1 ml 2 times/day for 10 days
4	Vehicle control	NA	E-PG (1:1)	Topical	50 μl 2 times/day for 10 days
5	Topical formulation 1	LSH001	Saturated drug solution in E-PG (1:1)	Topical	50 μl 2 times/day for 10 days
6	Topical formulation 2	LSH002	Saturated drug solution in E-PG (1:1)	Topical	50 μl 2 times/day for 10 days
7	Topical formulation 3	LSH003	Saturated drug solution in E-PG (1:1)	Topical	50 μl 2 times/day for 10 days
8	Oral formulation 1	LSH001	Standard suspended vehicle	Oral	25 mg/kg 2 times/day for 10 days
9	Oral formulation 2	LSH002	Standard suspended vehicle	Oral	25 mg/kg 2 times/day for 10 days
10	Oral formulation 3	LSH003	Standard suspended vehicle	Oral	25 mg/kg 2 times/day for 10 days

[a]b.i.d., twice a day; NA, not applicable.

lation conditions that would be used for topical dose administration in the murine model of CL. This *in vivo* study required a low application volume and a 1% (wt/vol) drug formulation.

For FDC studies, female BALB/c mouse skin was obtained from Bioreclamation IVT (Westbury, NY, USA) and stored at −80°C. On the day of each study, skin was thawed and hair was removed by careful clipping to avoid skin damage. Excess fat and muscle tissue was removed with the aid of a scalpel. Discs of skin approximately 2.5 cm in diameter were cut and mounted between the donor and receptor compartment of each FDC and kept in place by the use of a clamp. Vacuum silicone grease was applied to seal gaps and prevent leakage. The cells were left to equilibrate until the skin temperature stabilized at 32°C.

The donor and receptor solutions were prepared as described above. Receptor fluid samples were taken at time intervals over a period of 6 h. Each test compound was tested in triplicate. Statistical analysis was performed using SPSS software (version 19.0).

(ii) Mass balance during FDC studies. A mass balance study was conducted using the formulations and experimental conditions intended for use in the evaluation in the murine model of CL. The amount of drug that did not permeate into or through the skin (unabsorbed donor fraction) was obtained by gently swabbing the skin surface with a cotton bud at the end of the permeation experiment. This was repeated a second time. The cotton buds were placed in a tube with 1 ml of methanol (MeOH)-PBS (70:30) and left overnight on a shaker (800 rpm). An aliquot of the extraction fluid was analyzed by LC-MS/MS.

The Franz diffusion cells were dismantled, and the mouse skin was removed and placed in a vial. Three rounds of extraction with 1 ml of MeOH-PBS (7:3) were conducted. At each time, the vial was left to shake overnight before analysis by LC-MS/MS to extract the amount of drug that permeated into the skin. An acceptable mass balance was 80 to 120%, representing the total compound measured in the unabsorbed donor fraction, methanolic skin extracts, and the samples of receptor chamber fluid. Statistical analyses were performed using SPSS software (version 19.0).

Efficacy in a murine model of cutaneous leishmaniasis. (i) Drugs and formulation preparation. AmBisome, a liposomal formulation of amphotericin B for injection, was kindly provided by DNDi (Geneva, Switzerland) and prepared according to the manufacturer's recommendations. Briefly, AmBisome powder was reconstituted with 12 ml of cold sterile ultra-high-purity-grade water (>18 M$\Omega \cdot$ cm; Milli-Q water; Merck, Hertfordshire, UK) to produce a 4-mg/ml amphotericin B liposomal suspension. This suspension was vigorously shaken and incubated at 65°C for 10 min, after which it was allowed to cool to room temperature. This dispersion was diluted with sterile 5% (wt/vol) dextrose solution to obtain a final suspension of 0.5 mg of amphotericin B/ml. Every other day, up to 5 doses of 200 μl of this formulation were administered by bolus intravenous injection into a lateral tail vein. Leshcutan ointment, containing 15% paromomycin and 12% methylbenzethonium chloride (Teva, Israel), was purchased from Israelpharm.com, and 0.1 ml was applied with a 1-ml syringe and gently spread over the nodule twice daily for 10 days.

The experimental topical formulations containing compounds LSH001, LSH002, and LSH003 were prepared 24 h prior to the start of dosing. To allow maximal permeation, each test compound was applied as a saturated solution. An excess amount of the test compound was added to a 1:1 (vol/vol) mixture of propylene glycol (PG) and ethanol. The mixture was left to stir overnight, after which it was centrifuged at 15,668 × g for 15 min. The supernatant, i.e., a saturated solution, was pipetted into a clean vial, and 50 μl was applied to each mouse twice a day for 10 days (Table 8).

The standard suspension vehicle used to prepare the oral formulations was prepared by weighing and adding each component (0.5% [wt/vol] carboxymethyl cellulose, 0.5% [vol/vol] benzyl alcohol, and 0.4% [vol/vol] Tween 80 in a 0.9% [vol/vol] NaCl solution) into a clean glass vial. The mixture was left to stir overnight at room temperature prior to sterilization by autoclaving. The experimental oral formulations containing either LSH001, LSH002, or LSH003 in the vehicle were prepared by adding the appropriate amount of test compound to the vehicle in order to obtain a final concentration of 2.5 mg/ml. The suspension was sonicated for 30 min and was administered orally twice a day for 10 days. All formulations, including the AmBisome and topical formulations, were stored at 4°C throughout the experiment.

TABLE 9 Sequences of primers and probe targeting a 170-bp region of *Leishmania* species 18S rDNA used in the PCR and qPCRs

Primer or probe	Primer sequence
Forward primer	5′-C CAA AGT GTG GAG ATC GAA G-3′
Reverse primer	5′-GGC CGG TAA AGG CCG AAT AG-3′
Probe	5′-6FAM[a]-ACCATTGTAGTCCACACTGC-NFQ-MGB

[a]6FAM, 6-carboxyfluorescein.

(ii) Experimental CL model. Sixty female BALB/c mice (6 to 8 weeks old; Charles River Ltd., UK) were shaved on the rump above the tail and 1 day later injected with 2×10^7 stationary-phase *L. major* JISH118 promastigotes (200 μl) subcutaneously on the rump above the tail. At approximately 7 days postinfection, small nodules were visible. The nodule size was recorded daily, and when it reached an average diameter of 4.8 ± 0.8 mm, the mice were randomly allocated into groups of 6 mice each and drug administration was started. Formulations were administered over a period of 10 days. Untreated and topical vehicle-only control groups were included.

Treatment efficacy was evaluated by lesion size progression, measuring the lesion diameter in 2 dimensions on a daily basis using digital calipers (Jencons Scientific Ltd., UK). The average diameter was plotted as a function of time. Statistical analyses of differences between the average lesion diameter between groups on the last day of treatment were performed using one-way ANOVA with the Tukey *post hoc* test (SPSS software version 19.0). Three days after the end of treatment, the mice were sacrificed and the lesion was excised and stored at -80°C until the parasite load was quantified using real-time quantitative PCR (qPCR). Statistically significant differences in the average parasite numbers between different groups were analyzed using one-way ANOVA with the Tukey *post hoc* test (SPSS software, version 19.0).

(iii) Quantification of the parasite load in a CL lesion. On the day of extraction, the samples of lesion tissue were defrosted and cut into 2 approximately equal samples. One half was weighed and cut into fine pieces with a surgical blade before it was placed in a microcentrifuge tube. The proteinase K and lysis buffer were added to the tube, and samples were incubated at 56°C until a homogeneous mixture was obtained. The DNA of 200 μl of this homogenate was then extracted using a DNeasy blood and tissue kit (Qiagen) and eluted in the same volume. The purity and concentration of DNA were analyzed using a NanoDrop ND1000 spectrophotometer (Thermo Fisher Scientific).

The primer pair and probe, previously designed and validated by Van Der Meide et al. (71), targeted a 170-bp region in the *Leishmania* 18S ribosomal DNA (rDNA) gene and are specific for all *Leishmania* species. The respective sequences are shown in Table 9. Conventional PCR was performed to confirm the presence of the PCR product of the correct size and to verify primer efficacy. One microliter of a 1/100 dilution of the DNA extract was amplified in a final volume of 10 μl containing 2 μl of Kapa 2G buffer (Kapa Biosystems, Wilmington, MA) and primers at a concentration of 0.4 μM. The samples were run in a G-Storm GS4 machine (Somerset, UK). The amplification cycle started with a denaturation step at 95°C for 3 min, followed by 40 cycles of 95°C for 15 s, 60°C for 1 min, and 72°C for 30 s, with a final extension of 72°C for 30 s. Each run contained a negative sample whereby the extracted DNA was replaced by ultra-high-purity-grade water. The PCR products were separated on a 3% agarose gel, and the gel was stained with ethidium bromide and visualized under UV light. A 100-bp DNA ladder was run in parallel with the samples.

The parasite load was determined by means of quantitative PCR. For the amplification reaction, 2 μl of a 1/100-diluted DNA sample was added to 8 μl mix containing 5 μl Kapa Probe Fast qPCR master mix (2×; Kapa Biosystems, Wilmington, MA), 0.4 μM each primer, and 0.25 μM the appropriate probe. The tubes were placed in the 72-sample rotor of the instrument (Rotor Gene 3000; Qiagen), and the reaction with the following conditions was initiated: 95°C for 3 min, followed by 40 cycles of 95°C for 3 s and 60°C for 30 s. Each run contained a standard curve, a no-template control, and a negative control.

ACKNOWLEDGMENTS

REFERENCES

1. Alvar J, Velez ID, Bern C, Herrero M, Desjeux P, Cano J, Jannin J, den Boer M. 2012. Leishmaniasis worldwide and global estimates of its incidence. PLoS One 7:e35671. https://doi.org/10.1371/journal.pone.0035671.
2. Desjeux P. 2001. The increase in risk factors for leishmaniasis worldwide. Trans R Soc Trop Med Hyg 95:239–243. https://doi.org/10.1016/S0035-9203(01)90223-8.
3. Alirol E, Getaz L, Stoll B, Chappuis F, Loutan L. 2011. Urbanisation and infectious diseases in a globalised world. Lancet Infect Dis 11:131–141. https://doi.org/10.1016/S1473-3099(10)70223-1.
4. Rangel EF, da Costa SM, Carvalho BM. 2014. Environmental changes and the geographic spreading of American cutaneous leishmaniasis in Brazil. In Claborn D (ed), Leishmaniasis: trends in epidemiology, diagnosis and treatment. InTech, London, United Kingdom.
5. Hayani K, Dandashli A, Weisshaar E. 2015. Cutaneous leishmaniasis in

Syria: clinical features, current status and the effects of war. Acta Derm Venereol 95:62–66. https://doi.org/10.2340/00015555-1988.

6. Kassi M, Afghan A, Rehman R, Kasi PM. 2008. Marring leishmaniasis: the stigmatization and the impact of cutaneous leishmaniasis in Pakistan and Afghanistan. PLoS Negl Trop Dis 2:1–3. https://doi.org/10.1371/journal.pntd.0000259.

7. Alvar J, Croft S, Olliaro P. 2006. Chemotherapy in the treatment and control of leishmaniasis. Adv Parasitol 61:223–274. https://doi.org/10.1016/S0065-308X(05)61006-8.

8. De Rycker M, Hallyburton I, Thomas J, Campbell L, Wyllie S, Joshi D, Cameron S, Gilbert IH, Wyatt PG, Frearson JA, Fairlamb AH, Gray DW. 2013. Comparison of a high-throughput high-content intracellular Leishmania donovani assay with an axenic amastigote assay. Antimicrob Agents Chemother 57:2913–2922. https://doi.org/10.1128/AAC.02398-12.

9. Pena I, Pilar Manzano M, Cantizani J, Kessler A, Alonso-Padilla J, Bardera AI, Alvarez E, Colmenarejo G, Cotillo I, Roquero I, de Dios-Anton F, Barroso V, Rodriguez A, Gray DW, Navarro M, Kumar V, Sherstnev A, Drewry DH, Brown JR, Fiandor JM, Julio Martin J. 2015. New compound sets identified from high throughput phenotypic screening against three kinetoplastid parasites: an open resource. Sci Rep 5:8771. https://doi.org/10.1038/srep08771.

10. Carneiro G, Aguiar MG, Fernandes AP, Ferreira LA. 2012. Drug delivery systems for the topical treatment of cutaneous leishmaniasis. Expert Opin Drug Deliv 9:1083–1097. https://doi.org/10.1517/17425247.2012.701204.

11. Frankenburg S, Glick D, Klaus S, Barenholz Y. 1998. Efficacious topical treatment for murine cutaneous leishmaniasis with ethanolic formulations of amphotericin B. Antimicrob Agent Chemother 42:3092–3096.

12. Vardy D, Barenholz Y, Naftoliev N, Klaus S, Gilead L, Frankenburg S. 2001. Efficacious topical treatment for human cutaneous leishmaniasis with ethanolic lipid amphotericin B. Trans R Soc Trop Med Hyg 95:184–186. https://doi.org/10.1016/S0035-9203(01)90158-0.

13. Hussain A, Samad A, Nazish I, Ahmed FJ. 2014. Nanocarrier-based topical drug delivery for an antifungal drug. Drug Dev Ind Pharm 40:527–541. https://doi.org/10.3109/03639045.2013.771647.

14. Ruiz HK, Serrano DR, Dea-Ayuela MA, Bilbao-Ramos PE, Bolas-Fernandez F, Torrado JJ, Molero G. 2014. New amphotericin B-gamma cyclodextrin formulation for topical use with synergistic activity against diverse fungal species and Leishmania spp. Int J Pharm 473:148–157. https://doi.org/10.1016/j.ijpharm.2014.07.004.

15. El-On J, Jacobs GP, Witztum E, Greenblatt CL. 1984. Development of topical treatment for cutaneous leishmaniasis caused by Leishmania major in experimental animals. Antimicrob Agents Chemother 26:745–751. https://doi.org/10.1128/AAC.26.5.745.

16. El-On J, Jacobs GP, Weinrauch L. 1988. Topical chemotherapy of cutaneous Leishmaniasis. Parasitol Today 4:76–81. https://doi.org/10.1016/0169-4758(88)90200-1.

17. Carter KC, Alexander J, Baillie AJ. 1989. Studies on the topical treatment of experimental cutaneous leishmaniasis: the therapeutic effect of methyl benzethonium chloride and the aminoglycosides, gentamicin and paromomycin. Ann Trop Med Parasitol 83:233–239. https://doi.org/10.1080/00034983.1989.11812337.

18. Grogl M, Schuster BG, Ellis WY, Berman JD. 1999. Successful topical treatment of murine cutaneous leishmaniasis with a combination of paromomycin (Aminosidine) and gentamicin. J Parasitol 85:354–359. https://doi.org/10.2307/3285646.

19. Ferreira LS, Ramaldes GA, Nunan EA, Ferreira LA. 2004. In vitro skin permeation and retention of paromomycin from liposomes for topical treatment of cutaneous leishmaniasis. Drug Dev Ind Pharm 30:289–296. https://doi.org/10.1081/DDC-120030423.

20. Van Bocxlaer K, Yardley V, Murdan S, Croft SL. 2016. Drug permeation and barrier damage in Leishmania-infected mouse skin. J Antimicrob Chemother 71:1578–1585. https://doi.org/10.1093/jac/dkw012.

21. Croft SL, Seifert K, Yardley V. 2006. Current scenario of drug development for leishmaniasis. Indian J Med Res 123:399–410.

22. Jacobs RT, Plattner JJ, Keenan M. 2011. Boron-based drugs as antiprotozoals. Curr Opin Infect Dis 24:586–592. https://doi.org/10.1097/QCO.0b013e32834c630e.

23. Zhang YK, Plattner JJ, Freund YR, Easom EE, Zhou Y, Gut J, Rosenthal PJ, Waterson D, Gamo FJ, Angulo-Barturen I, Ge M, Li Z, Li L, Jian Y, Cui H, Wang H, Yang J. 2011. Synthesis and structure-activity relationships of novel benzoxaboroles as a new class of antimalarial agents. Bioorg Med Chem Lett 21:644–651. https://doi.org/10.1016/j.bmcl.2010.12.034.

24. Zhang YK, Plattner JJ, Freund YR, Easom EE, Zhou Y, Ye L, Zhou H, Waterson D, Gamo FJ, Sanz LM, Ge M, Li Z, Li L, Wang H, Cui H. 2012. Benzoxaborole antimalarial agents. Part 2: discovery of fluoro-substituted 7-(2-carboxyethyl)-1,3-dihydro-1-hydroxy-2,1-benzoxaboroles. Bioorg Med Chem Lett 22:1299–1307. https://doi.org/10.1016/j.bmcl.2011.12.096.

25. Jacobs RT, Plattner JJ, Nare B, Wring SA, Chen D, Freund Y, Gaukel EG, Orr MD, Perales JB, Jenks M, Noe RA, Sligar JM, Zhang YK, Bacchi CJ, Yarlett N, Don R. 2011. Benzoxaboroles: a new class of potential drugs for human African trypanosomiasis. Future Med Chem 3:1259–1278. https://doi.org/10.4155/fmc.11.80.

26. Hu Q-H, Liu R-J, Fang Z-P, Zhang J, Ding Y-Y, Tan M, Wang M, Pan W, Zhou H-C, Wang E-D. 2013. Discovery of a potent benzoxaborole-based anti-pneumococcal agent targeting leucyl-tRNA synthetase. Sci Rep 3:2475. https://doi.org/10.1038/srep02475.

27. Liu CT, Tomsho JW, Benkovic SJ. 2014. The unique chemistry of benzoxaboroles: current and emerging applications in biotechnology and therapeutic treatments. Bioorg Med Chem 22:4462–4473. https://doi.org/10.1016/j.bmc.2014.04.065.

28. Nare B, Wring S, Bacchi C, Beaudet B, Bowling T, Brun R, Chen D, Ding C, Freund Y, Gaukel E, Hussain A, Jarnagin K, Jenks M, Kaiser M, Mercer L, Mejia E, Noe A, Orr M, Parham R, Plattner J, Randolph R, Rattendi D, Rewerts C, Sligar J, Yarlett N, Don R, Jacobs R. 2010. Discovery of novel orally bioavailable oxaborole 6-carboxamides that demonstrate cure in a murine model of late-stage central nervous system African trypanosomiasis. Antimicrob Agents Chemother 54:4379–4388. https://doi.org/10.1128/AAC.00498-10.

29. Irvine JD, Takahashi L, Lockhart K, Cheong J, Tolan JW, Selick HE, Grove JR. 1999. MDCK (Madin-Darby canine kidney) cells: a tool for membrane permeability screening. J Pharm Sci 88:28–33. https://doi.org/10.1021/js9803205.

30. Thiel-Demby VE, Humphreys JE, St John Williams LA, Ellens HM, Shah N, Ayrton AD, Polli JW. 2009. Biopharmaceutics classification system: validation and learnings of an in vitro permeability assay. Mol Pharm 6:11–18. https://doi.org/10.1021/mp800122b.

31. Costa IS, de Souza GF, de Oliveira MG, Abrahamsohn IDA. 2013. S-nitrosoglutathione (GSNO) is cytotoxic to intracellular amastigotes and promotes healing of topically treated Leishmania major or Leishmania braziliensis skin lesions. J Antimicrob Chemother 68:2561–2568. https://doi.org/10.1093/jac/dkt210.

32. DNDi. 2016. DNDi portfolio June 2016. DNDi, Geneva, Switzerland. http://www.dndi.org/diseases-projects/portfolio/. Accessed 15 March 2017.

33. Bos JD, Meinardi MM. 2000. The 500 dalton rule for the skin penetration of chemical compounds and drugs. Exp Dermatol 9:165–169. https://doi.org/10.1034/j.1600-0625.2000.009003165.x.

34. Hadgraft J, Pugh WJ. 1998. The selection and design of topical and transdermal agents: a review. J Investig Dermatol Symp Proc 3:131–135. https://doi.org/10.1038/jidsymp.1998.27.

35. Choy YB, Prausnitz MR. 2011. The rule of five for non-oral routes of drug delivery: ophthalmic, inhalation and transdermal. Pharm Res 28:943–948. https://doi.org/10.1007/s11095-010-0292-6.

36. Vecchia BE, Bunge AL. 2002. Evaluating the transdermal permeability of chemicals. In transdermal drug delivery systems. CRC Press LLC, Boca Raton, FL.

37. Naik A, Kalia YN, Guy RH. 2000. Transdermal drug delivery: overcoming the skin's barrier function. Pharm Sci Technol Today 3:318–326. https://doi.org/10.1016/S1461-5347(00)00295-9.

38. Roberts MS, Pugh WJ, Hadgraft J. 1996. Epidermal permeability: penetrant structure relationships 0.2. The effect of H-bonding groups in penetrants on their diffusion through the stratum corneum. Int J Pharm 132:23–32.

39. Brody I. 1977. Ultrastructure of the stratum corneum. Int J Dermatol 16:245–256. https://doi.org/10.1111/j.1365-4362.1977.tb04315.x.

40. Downing DT, Stewart ME, Wertz PW, Colton SW, Strauss JS. 1983. Skin lipids. Comp Biochem Physiol B 76:673–678.

41. Neal RA, Croft SL. 1984. An in-vitro system for determining the activity of compounds against the intracellular amastigote form of Leishmania donovani. J Antimicrob Chemother 14:463–475. https://doi.org/10.1093/jac/14.5.463.

42. Thiel-Demby VE, Tippin TK, Humphreys JE, Serabjit-Singh CJ, Polli JW. 2004. In vitro absorption and secretory quotients: practical criteria derived from a study of 331 compounds to assess for the impact of

P-glycoprotein-mediated efflux on drug candidates. J Pharm Sci 93: 2567–2572. https://doi.org/10.1002/jps.20166.

43. Mahar Doan KM, Wring SA, Shampine LJ, Jordan KH, Bishop JP, Kratz J, Yang E, Serabjit-Singh CJ, Adkison KK, Polli JW. 2004. Steady-state brain concentrations of antihistamines in rats: interplay of membrane permeability, P-glycoprotein efflux and plasma protein binding. Pharmacology 72:92–98. https://doi.org/10.1159/000079137.

44. Evers R, Kool M, Smith AJ, van Deemter L, de Haas M, Borst P. 2000. Inhibitory effect of the reversal agents V-104, GF120918 and Pluronic L61 on MDR1 Pgp-, MRP1- and MRP2-mediated transport. Br J Cancer 83:366–374. https://doi.org/10.1054/bjoc.2000.1260.

45. Tran TT, Mittal A, Aldinger T, Polli JW, Ayrton A, Ellens H, Bentz J. 2005. The elementary mass action rate constants of P-gp transport for a confluent monolayer of MDCKII-hMDR1 cells. Biophys J 88:715–738. https://doi.org/10.1529/biophysj.104.045633.

46. Acharya P, O'Connor MP, Polli JW, Ayrton A, Ellens H, Bentz J. 2008. Kinetic identification of membrane transporters that assist P-glycoprotein-mediated transport of digoxin and loperamide through a confluent monolayer of MDCKII-hMDR1 cells. Drug Metab Dispos 36: 452–460. https://doi.org/10.1124/dmd.107.017301.

47. Janneh O, Jones E, Chandler B, Owen A, Khoo SH. 2007. Inhibition of P-glycoprotein and multidrug resistance-associated proteins modulates the intracellular concentration of lopinavir in cultured CD4 T cells and primary human lymphocytes. J Antimicrob Chemother 60:987–993. https://doi.org/10.1093/jac/dkm353.

48. Jovelet C, Deroussent A, Broutin S, Paci A, Farinotti R, Bidart JM, Gil S. 2013. Influence of the multidrug transporter P-glycoprotein on the intracellular pharmacokinetics of vandetanib. Eur J Drug Metab Pharmacokinet 38:149–157. https://doi.org/10.1007/s13318-013-0123-3.

49. Lemaire S, Van Bambeke F, Mingeot-Leclercq MP, Tulkens PM. 2007. Modulation of the cellular accumulation and intracellular activity of daptomycin towards phagocytized Staphylococcus aureus by the P-glycoprotein (MDR1) efflux transporter in human THP-1 macrophages and Madin-Darby canine kidney cells. Antimicrob Agents Chemother 51:2748–2757. https://doi.org/10.1128/AAC.00090-07.

50. Seral C, Carryn S, Tulkens PM, Van Bambeke F. 2003. Influence of P-glycoprotein and MRP efflux pump inhibitors on the intracellular activity of azithromycin and ciprofloxacin in macrophages infected by Listeria monocytogenes or Staphylococcus aureus. J Antimicrob Chemother 51:1167–1173. https://doi.org/10.1093/jac/dkg223.

51. Mookerjee Basu J, Mookerjee A, Banerjee R, Saha M, Singh S, Naskar K, Tripathy G, Sinha PK, Pandey K, Sundar S, Bimal S, Das PK, Choudhuri SK, Roy S. 2008. Inhibition of ABC transporters abolishes antimony resistance in Leishmania infection. Antimicrob Agents Chemother 52: 1080–1093. https://doi.org/10.1128/AAC.01196-07.

52. Alvarez-Figueroa MJ, Pessoa-Mahana CD, Palavecino-Gonzalez ME, Mella-Raipan J, Espinosa-Bustos C, Lagos-Munoz ME. 2011. Evaluation of the membrane permeability (PAMPA and skin) of benzimidazoles with potential cannabinoid activity and their relation with the Biopharmaceutics Classification System (BCS). AAPS PharmSciTech 12:573–578. https://doi.org/10.1208/s12249-011-9622-1.

53. Schreiber S, Mahmoud A, Vuia A, Rubbelke MK, Schmidt E, Schaller A, Kandarova H, Haberland A, Schafer UF, Bock U, Korting HC, Liebsch A, Schafer-Korting A. 2005. Reconstructed epidermis versus human and animal skin in skin absorption studies. Toxicol In Vitro 19:813–822. https://doi.org/10.1016/j.tiv.2005.04.004.

54. Schafer-Korting M, Bock U, Gamer A, Haberland A, Haltner-Ukomadu E, Kaca M, Kamp H, Kietzmann M, Korting HC, Krachter HU, Lehr CM, Liebsch M, Mehling A, Netzlaff F, Niedorf F, Rubbelke MK, Schafer U, Schmidt E, Schreiber S, Schroder KR, Spielmann H, Vuia A. 2006. Reconstructed human epidermis for skin absorption testing: results of the German prevalidation study. Altern Lab Anim 34:283–294.

55. Lotte C, Patouillet C, Zanini M, Messager A, Roguet R. 2002. Permeation and skin absorption: reproducibility of various industrial reconstituted

human skin models. Skin Pharmacol Physiol 15(Suppl 1):18–30. https://doi.org/10.1159/000066679.

56. Kao J, Patterson FK, Hall J. 1985. Skin penetration and metabolism of topically applied chemicals in six mammalian species, including man: an in vitro study with benzo[a]pyrene and testosterone. Toxicol Appl Pharmacol 81:502–516. https://doi.org/10.1016/0041-008X(85)90421-1.

57. Muller B, Kasper M, Surber C, Imanidis G. 2003. Permeation, metabolism and site of action concentration of nicotinic acid derivatives in human skin. Correlation with topical pharmacological effect. Eur J Pharm Sci 20:181–195.

58. Morris AP, Brain KR, Heard CM. 2009. Skin permeation and ex vivo skin metabolism of O-acyl haloperidol ester prodrugs. Int J Pharm 367:44–50. https://doi.org/10.1016/j.ijpharm.2008.09.013.

59. Montagna W. 1955. Histology and cytochemistry of human skin. IX. The distribution of non-specific esterases. J Biophys Biochem Cytol 1:13–16. https://doi.org/10.1083/jcb.1.1.13.

60. Ozaki H, Sugihara K, Watanabe Y, Fujino C, Uramaru N, Sone T, Ohta S, Kitamura S. 2013. Comparative study of the hydrolytic metabolism of methyl-, ethyl-, propyl-, butyl-, heptyl- and dodecylparaben by microsomes of various rat and human tissues. Xenobiotica 43:1064–1072. https://doi.org/10.3109/00498254.2013.802059.

61. Bonina FP, Puglia C, Barbuzzi T, de Caprariis P, Palagiano F, Rimoli MG, Saija A. 2001. In vitro and in vivo evaluation of polyoxyethylene esters as dermal prodrugs of ketoprofen, naproxen and diclofenac. Eur J Pharm Sci 14:123–134. https://doi.org/10.1016/S0928-0987(01)00163-4.

62. Harville HM, Voorman R, Prusakiewicz JJ. 2007. Comparison of paraben stability in human and rat skin. Drug Metab Lett 1:17–21. https://doi.org/10.2174/187231207779814300.

63. Gonzalez D, Schmidt S, Derendorf H. 2013. Importance of relating efficacy measures to unbound drug concentrations for anti-infective agents. Clin Microbiol Rev 26:274–288. https://doi.org/10.1128/CMR.00092-12.

64. Yardley V, Croft SL. 1999. Animal models of cutaneous leishmaniasis, p 775–781. In Zak O (ed), Handbook of animals of infection. Academic Press, London, United Kingdom.

65. Coelho AC, Trinconi CT, Costa CH, Uliana SR. 2014. In vitro and in vivo miltefosine susceptibility of a Leishmania amazonensis isolate from a patient with diffuse cutaneous leishmaniasis. PLoS Negl Trop Dis 8:e2999. https://doi.org/10.1371/journal.pntd.0002999.

66. Katsuno K, Burrows JN, Duncan K, Hooft van Huijsduijnen R, Kaneko T, Kita K, Mowbray CE, Schmatz D, Warner P, Slingsby BT. 2015. Hit and lead criteria in drug discovery for infectious diseases of the developing world. Nat Rev Drug Discov 14:751–758. https://doi.org/10.1038/nrd4683.

67. Grogl M, Hickman M, Ellis W, Hudson T, Lazo JS, Sharlow ER, Johnson J, Berman J, Sciotti RJ. 2013. Drug discovery algorithm for cutaneous leishmaniasis. Am J Trop Med Hyg 88:216–221. https://doi.org/10.4269/ajtmh.11-0812.

68. Edwards JE, Brouwer KR, McNamara PJ. 2002. GF120918, a P-glycoprotein modulator, increases the concentration of unbound amprenavir in the central nervous system in rats. Antimicrob Agents Chemother 46:2284–2286. https://doi.org/10.1128/AAC.46.7.2284-2286.2002.

69. Troutman MD, Thakker DR. 2003. Novel experimental parameters to quantify the modulation of absorptive and secretory transport of compounds by P-glycoprotein in cell culture models of intestinal epithelium. Pharm Res 20:1210–1224. https://doi.org/10.1023/A:1025001131513.

70. Mahjour M, Mauser BE, Rashidbaigi ZA, Fawzi MB. 1993. Effects of propylene glycol diesters of caprylic and capric acids (Miglyol® 840) and ethanol binary systems on in vitro skin permeation of drugs. Int J Pharm 95:161–169. https://doi.org/10.1016/0378-5173(93)90403-3.

71. van der Meide W, Guerra J, Schoone G, Farenhorst M, Coelho L, Faber W, Peekel I, Schallig H. 2008. Comparison between quantitative nucleic acid sequence-based amplification, real-time reverse transcriptase PCR, and real-time PCR for quantification of Leishmania parasites. J Clin Microbiol 46:73–78. https://doi.org/10.1128/JCM.01416-07.